

## Research Article

# Direct Benzyl Alcohol and Benzaldehyde Synthesis from Toluene over Keggin-Type Polyoxometalates Catalysts: Kinetic and Mechanistic Studies

Allam Djaouida, Mansouri Sadia, and Hocine Smaïn 

Laboratoire de Génie Chimique et Chimie Appliquée Hasnaoua I, Université de Mouloud Mammeri, BP. 17 RP 15000 Tizi-Ouzou, Algeria

Correspondence should be addressed to Hocine Smaïn; [shocine\\_univ\\_to@yahoo.fr](mailto:shocine_univ_to@yahoo.fr)

Received 8 September 2018; Accepted 12 November 2018; Published 13 January 2019

Academic Editor: Fateme Razeai

Copyright © 2019 Allam Djaouida et al. This is an open access article distributed under the Creative Commons Attribution License, which permits unrestricted use, distribution, and reproduction in any medium, provided the original work is properly cited.

The catalytic activity of various Keggin polyoxometalate catalysts has been investigated in the gas-phase partial oxidation of toluene to produce benzyl alcohol and benzaldehyde. The catalyst systems  $\text{HPMo}_{12}\text{O}_{40}$ ,  $\text{HPMo}_{11}\text{VO}_{40}$ ,  $\text{FePMo}_{12}\text{O}_{40}$ , and  $\text{PMo}_{11}\text{FeO}_{39}$  were prepared and characterized by FT-IR, UV-visible, SEM, XRD, TGA, and cyclic voltammetry. The acid/base properties were evaluated using the decomposition of isopropanol. Catalytic studies were carried under atmospheric pressure and over the temperature range  $200^{\circ}\text{C}$ – $350^{\circ}\text{C}$ , using carbon dioxide as a mild oxidant. Toluene conversion and product distribution depend mainly on the catalyst composition and operating conditions. In addition to benzaldehyde, benzyl alcohol is obtained with a high selectivity on the  $\text{PMo}_{11}\text{FeO}_{39}$  catalyst. The kinetic data show that the reoxidation of the reduced catalyst is the rate-limiting step for the partial oxidation reaction of toluene.

## 1. Introduction

Aromatic aldehydes such as benzaldehyde are very valuable industrial organic intermediates, and their uses include the manufacture of flavors, fragrances, pharmaceutical precursors, and plastic additives. Industrially, benzaldehyde is produced exclusively by the liquid phase oxidation of toluene [1, 2]. Usually, benzaldehyde is made by a process in which toluene is treated with chlorine to form benzal chloride, followed by treatment of benzal chloride with water. This process suffers from several problems, such as the formation of undesirable products, equipment corrosion with chlorine, and complex products' separation. An alternative is the gas-phase oxidation of toluene. However, toluene conversion and product distribution largely depended on catalyst composition and operating conditions. Vanadium oxide-based materials are the most commonly used catalysts in this process. Since the discovery of the effectiveness of vanadium pentoxide as catalyst in sulfur dioxide oxidation by Haen [3], in 1900, a considerable number of studies have been carried in homogeneous and

heterogeneous catalysis, such as the conversion of alkanes to the corresponding alkenes [4–7] and the conversion of alcohols to aldehydes or ketones [8–11]. Supported vanadium oxide catalysts are also used in gas-phase catalytic partial oxidation of toluene [12–14]. The supported vanadium-based catalysts were reported to show high benzaldehyde selectivity, but the toluene conversion was below 10% at the low temperature ( $<400^{\circ}\text{C}$ ). However, at higher temperature ( $>400^{\circ}\text{C}$ ), the toluene conversion increased and the selectivity to benzaldehyde decreased and those to carbon oxides increased. Other workers have reported that pure and mixed molybdenum oxides are very efficient in gas-phase partial oxidation of toluene [15]. The main reaction products were maleic anhydride, benzaldehyde, and carbon oxides [16]. The investigation of the influence of various metal oxides on the behaviour of molybdenum oxide towards the oxidation of toluene with molecular oxygen concluded that toluene oxidation decreases in the following order: support oxides  $\geq$  molybdenum oxide monolayer catalysts  $>$  molybdate salts  $>$  crystalline molybdenum oxide, but the benzaldehyde and

benzoic acid selectivities follow the opposite trend [15]. Although there is a large number of catalysts described in the literature and in the patent literature composed of the vanadium oxides systems modified by various promoters, supported on carriers  $\text{Al}_2\text{O}_3$ ,  $\text{SiO}_2$ ,  $\text{TiO}_2$ , and transition metal oxides and favorable for the catalytic gas-phase toluene oxidation to benzaldehyde [17–24], but the toluene conversion is very poor at low temperature (less than 10%). This catalyst system favors the formation of benzoic acid and degradation of carbon dioxide and benzaldehyde selectivity is not very satisfactory. Therefore, a suitable catalyst for the selective production of benzaldehyde from toluene is strongly desired. More attention has been given to the application of the polyoxometalates having Keggin structure, as catalysts for the oxydehydrogenation of alkanes to alkenes [24–27]. Keggin-type polyoxometalates have been widely used as catalysts for one-step conversion of lower alkanes into value-added oxygenated products, such as partial oxidation of methane to methanol [28], oxidation of isobutane to methacrylic acid (MAA) [29], and partial oxidation of propane to acrylic acid (AA) [30]. Molecular oxygen was first proposed to be the oxidizing agent. However, it appeared that use of  $\text{O}_2$  (strong oxidant) leads to complete oxidation of hydrocarbons to  $\text{CO}_x$ . As an alternative to the strong oxidant  $\text{O}_2$ , carbon dioxide, the main contributor to the greenhouse effect, was proposed as nontraditional mild oxidant for catalytic oxidation of light alkanes [31–33].  $\text{CO}_2$  utilization as a mild oxidant and an oxygen transfer agent is attracting considerable attention and considered as another route for increasing selectivity and to avoid total oxidation [34]. This approach is expected to open new technology for  $\text{CO}_2$  utilization.

In this paper, heteropolyacids  $\text{H}_3\text{PMo}_{12}\text{O}_{40}$  ( $\text{HPMo}_{12}$ ) and  $\text{H}_4\text{PMo}_{11}\text{VO}_{40}$  ( $\text{HPMo}_{11}\text{V}$ ) and heteropolysalts  $(\text{NH}_4)_{2.5}\text{Fe}_{0.1}\text{H}_{0.2}\text{PMo}_{12}\text{O}_{40}$  ( $\text{FePMo}_{12}$ ) and  $(\text{NH}_4)_4\text{PMo}_{11}(\text{H}_2\text{O})\text{FeO}_{39}$  ( $\text{PMo}_{11}\text{Fe}$ ) were prepared, characterized by different methods (FT-IR, UV-visible, MEB, XRD, TGA, and cyclic voltammetry), and the acid/base properties were evaluated using the isopropanol decomposition. The catalytic performance of the catalysts was investigated in partial oxidation of toluene in the temperature range  $200^\circ\text{C}$ – $350^\circ\text{C}$  at atmospheric pressure using carbon dioxide as oxidant. The reaction mechanism and kinetics are discussed. The kinetic study was carried over  $\text{PMo}_{11}\text{Fe}$  catalyst at  $200^\circ\text{C}$ .

## 2. Experimental

**2.1. Catalyst Preparation.** Pure heteropolyacids  $\text{H}_3\text{PMo}_{12}\text{O}_{40}$  and  $\text{H}_4\text{PMo}_{11}\text{VO}_{40}$  samples were prepared in a classical way [35]. The ammonium-iron salt,  $(\text{NH}_4)_{2.5}\text{Fe}_{0.1}\text{H}_{0.2}\text{PMo}_{12}\text{O}_{40}$ , was prepared by adding  $(\text{NH}_4)_2\text{CO}_3$  solution to an aqueous solution of mixture of  $\text{H}_3\text{PMo}_{12}\text{O}_{40}$  and  $\text{Fe}(\text{NO}_3)_3$ . The precipitate was dried at  $50^\circ\text{C}$  under vacuum for 5 h.  $(\text{NH}_4)_4\text{PMo}_{11}\text{FeO}_{39}$  salt was prepared by the method described in the literature [36]. The paramolybdate of ammonium was dissolved at  $50^\circ\text{C}$ . The mixture of  $\text{H}_3\text{PO}_4$ ,  $\text{HNO}_3$ , and  $\text{Fe}(\text{NO}_3)_3$  was introduced slowly in the aqueous solution of ammonium paramolybdate at  $0^\circ\text{C}$ . Salt of ammonium was precipitated immediately by ammonium nitrates ( $\text{NH}_4\text{NO}_3$ ).

**2.2. Characterization.** Fourier transform infrared spectra (FT-IR) of the heteropolycompounds were obtained in the  $400$ – $4000\text{ cm}^{-1}$  wavenumber range using a FTIR-8400 Shimadzu spectrometer. UV-vis spectra were recorded on a UV-vis scanning spectrophotometer (Shimadzu UV-2100PC). A  $2.5\text{ mM}$  reaction solution of each catalyst was sampled, and the solution was diluted with  $400\text{ ml}$  acetonitrile ( $0.5\text{ mM}$ ). Then, the UV-vis spectrum of the solution was measured at  $25^\circ\text{C}$ .

The X-ray diffraction (XRD) patterns were obtained on a Siemens “D5000” diffractometer with  $\text{Cu K}\alpha$  radiation. The diffractograms were registered at Bragg angle ( $2\theta$ ) =  $5$ – $45^\circ$  at a scan rate of  $5^\circ/\text{min}$ . The thermal decomposition of heteropolycompounds was studied using a Setaram TG-DTA 92.  $20\text{ mg}$  of powder was placed in the sample holder, and the temperature was elevated at  $5^\circ\text{C}/\text{min}$  in flowing synthetic air.

Isopropanol decomposition and cyclic voltammetry are used to know the information about the redox properties of the heteropolyanions.

The isopropanol decomposition was carried out at atmospheric pressure, in a conventional flow fixed-bed reactor, using  $0.2\text{ g}$  of catalyst. Nitrogen was the carrier gas with a flow rate of  $50\text{ mL}/\text{min}$ . The reaction products were quantified by gas chromatography, using an FID and TC detector.

**2.3. Catalytic Tests.** Catalytic tests were carried out at atmospheric pressure in a continuous flow fixed-bed tubular glass reactor with  $1\text{ g}$  of catalyst pretreated in nitrogen ( $2\text{ L}/\text{h}$ ) for  $1\text{ h}$  at the reaction temperature. The carbon dioxide stream ( $2\text{ L}/\text{h}$ ) was saturated with toluene ( $50\text{ Torr}$ ). The oxydehydrogenation (ODH) of toluene was carried out at a relatively lower temperature,  $250^\circ\text{C}$ – $350^\circ\text{C}$ , in which the carbon formation is thermodynamically unflavored. The reaction mixture (toluene, benzaldehyde, benzene, benzyl alcohol, methane, and  $\text{CO}$ ) was analyzed by a gas chromatograph (DTC and FID CG, Shimadzu 14B) equipped with columns of Molecular Sieve 5A and Porapak QS.

## 3. Results and Discussion

### 3.1. Results of Characterization

**3.1.1. FT-IR Analysis.** IR spectra of all compounds are given in Figure 1. The characteristic peaks of Keggin unit were observed in the region  $1100$ – $500\text{ cm}^{-1}$ . According to literature data [37], the origin of the Keggin anion vibration bands, appearing at  $1065$ ,  $961$ ,  $864$ , and  $789\text{ cm}^{-1}$ , is attributed to  $\text{P-O}_a$ ,  $\text{Mo=O}_t$ , interoctahedral  $\text{Mo-O}_b$ - $\text{Mo}$ , and intraoctahedral  $\text{Mo-O}_c$ - $\text{Mo}$  bands, respectively. The FT-IR spectra presented in Figure 1 showed splitting of  $\text{P-O}_a$  band of value equal to  $40\text{ cm}^{-1}$  for  $\text{PMo}_{11}\text{V}$  and  $24\text{ cm}^{-1}$  for  $\text{PMo}_{11}\text{Fe}$ ; the result showed clearly that vanadium and iron ions were introduced into octahedral position. There is no apparent difference between the  $\text{PMo}_{12}$  and  $\text{FePMo}_{12}$  spectra; we can note from the results that the primary Keggin structure remains unaltered even when the protons from parental heteropolyacid are substituted by the ammonium and iron cations. The absorption band around  $1600\text{ cm}^{-1}$  is indicative of the presence of oxonium ions ( $\text{H}_3\text{O}^+$ ) or more

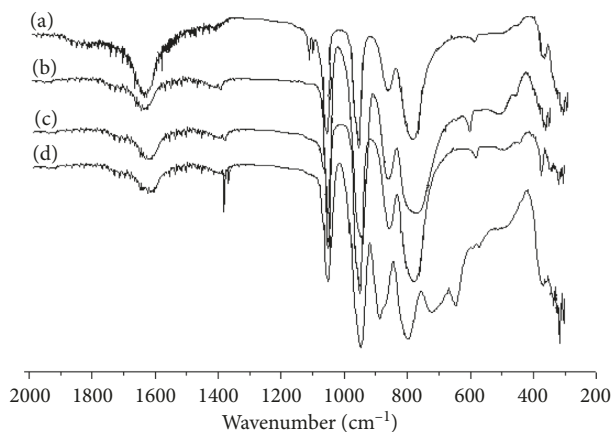


FIGURE 1: FTIR spectra of (a)  $\text{HPMo}_{12}$ ; (b)  $\text{FePMo}_{12}$ ; (c)  $\text{HPMo}_{11}\text{V}$ ; (d)  $\text{PMo}_{11}\text{Fe}$ .

likely to dioxonium ions ( $\text{H}_5\text{O}_2^+$ ). The band at  $1420\text{ cm}^{-1}$  was assigned to N–H stretching.

**3.1.2. UV-Visible Analysis.** In the near UV, the electronic spectra of Keggin-type polyoxometalates show two absorption bands around 220 nm and 300 nm (Figure 2). These bands attributed to metal oxygen charge transfer. According to the literature [37], these bands are assigned, respectively, to the vibrations of Mo–Ot bonds and Mo–Ob/Oc.

**3.1.3. XRD Analysis.** As shown in Figure 3, the XRD patterns of  $\text{HPMo}_{12}\text{O}_{40}$  and  $\text{HPMo}_{11}\text{VO}_{40}$  were substantially similar and have a Keggin-type structure. The acidic  $\text{HPMo}_{12}\text{O}_{40}$  and  $\text{HPMo}_{11}\text{VO}_{40}$  crystallize in the triclinic system, with  $a = 14.10\text{ \AA}$ ,  $b = 14.13\text{ \AA}$ ,  $c = 13.39\text{ \AA}$ ,  $\alpha = 112.1^\circ$ ,  $\beta = 109.8^\circ$ ,  $\gamma = 60.73^\circ$  and  $a = 14.04\text{ \AA}$ ,  $b = 10.006\text{ \AA}$ ,  $c = 13.55\text{ \AA}$  and  $\alpha = 112^\circ$ ,  $\beta = 109.58^\circ$ ,  $\gamma = 60.72^\circ$ , respectively.

The diffraction patterns of  $\text{FePMo}_{12}$  shown in Figure 3 indicate for the compound the existence of a single crystallographic phase with patterns typical of a cubic phase (intense peak corresponding to [222] plane) (space group  $I m\bar{3}$ ) with  $a = b = c = 11.6812$ ,  $Z = 2$ .

X-ray analysis of  $(\text{NH}_4)_4\text{PMo}_{11}\text{Fe}(\text{H}_2\text{O})\text{O}_{39}\cdot x\text{H}_2\text{O}$  showed that it crystallizes in the monoclinic system, space group  $P 2_1/c$ , with,  $a = 20,07210\text{ \AA}$ ,  $b = 11,55938\text{ \AA}$ ,  $c = 18,77828\text{ \AA}$ ,  $\beta = 95,664^\circ$ , and  $Z = 2$ .

**3.1.4. SEM Analysis.** The scanning electron micrographs of heteropolycompound catalysts are shown in Figure 4. These images show that the morphology of the particles depends on the heteropolycompound composition and content. The principle structure of  $\text{FePMo}_{12}$  and  $\text{PMo}_{11}\text{Fe}$  was the same and consisted of rosette-shape plate-like crystals. The particles of  $\text{HPMo}_{12}$  differ from that of  $\text{HPMo}_{11}\text{V}$  in morphology. The samples of both catalysts contain particles with nonuniform size and shape.

**3.1.5. Voltamperometric Analysis.** The redox properties of heteropolyanions have been studied by cyclic voltammetry. Keggin anions are able to accept reversibly up to six electrons

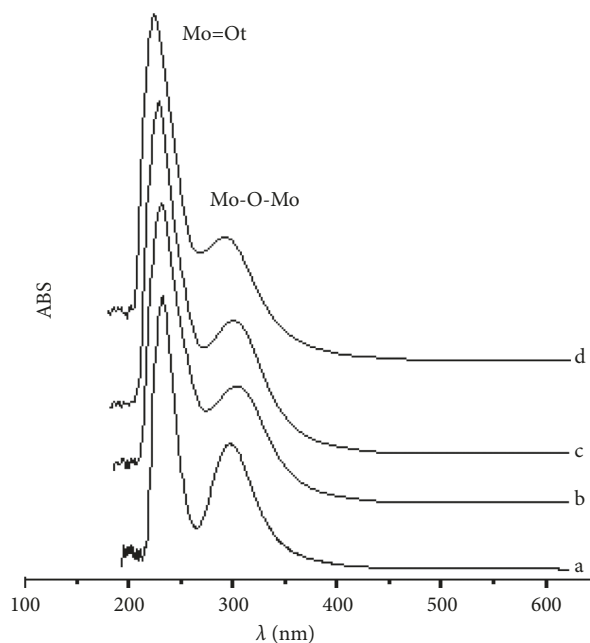


FIGURE 2: UV-visible absorption spectra of (a)  $\text{PMo}_{11}\text{Fe}$ ; (b)  $\text{FePMo}_{12}$ ; (c)  $\text{HPMo}_{12}$ ; (d)  $\text{HPMo}_{11}\text{V}$ .

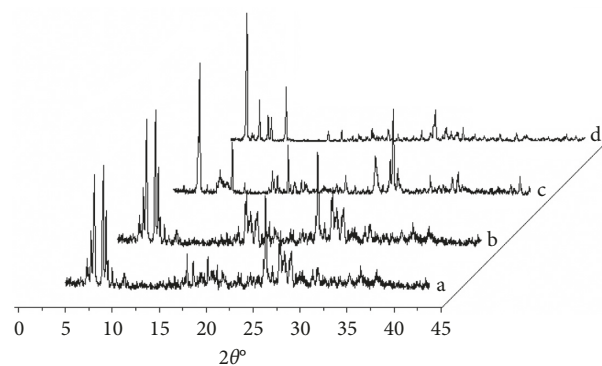


FIGURE 3: XRD patterns of (a)  $\text{HPMo}_{12}$ ; (b)  $\text{HPMo}_{11}\text{V}$ ; (c)  $\text{PMo}_{11}\text{Fe}$ ; (d)  $\text{FePMo}_{12}$ .

on the vanadium, molybdenum, or tungsten atoms and thus are potential oxidants. Figure 5(a) shows a cyclic voltammogram of  $0.50\text{ mM } [\text{PMo}_{12}\text{O}_{40}]^{3-}$  anion in acetonitrile/water (ratio 1/1 by volume), using a glassy carbon rotating electrode. Three-step, one-electron redox wave was obtained with midpoint potentials,  $E_{\text{mid}}$  of  $-0.75$ ,  $-0.4$ , and  $-0.05\text{ V}$  assigned to the successive reduction molybdenum centers, where  $E_{\text{mid}} = (E_{\text{pc}} - E_{\text{pa}})/2$ ;  $E_{\text{pc}}$  and  $E_{\text{pa}}$  are the cathodic and the anodic peak potentials, respectively. The same result is observed with iron-substituted heteropolymolybdate ( $\text{FePMo}_{12}$ ).

Cyclic Voltammetry studies of  $\text{HPMo}_{11}\text{V}$  and  $\text{PMo}_{11}\text{Fe}$  were particularly informative. Figures 5(c) and 5(d) show typical cyclic voltammograms for the anions  $(\text{HPMo}_{11}\text{VO}_{40})^{4-}$  and  $(\text{PMo}_{11}\text{FeO}_{39})^{7-}$ . The number of redox processes identified and the values of the peak potentials are quite similar. It consists of a reversible one-electron system at  $-0.11$  and  $-0.7\text{ V}$  for the  $\text{HPMo}_{11}\text{V}$  and for  $\text{PMo}_{11}\text{Fe}$ , respectively, assigned to

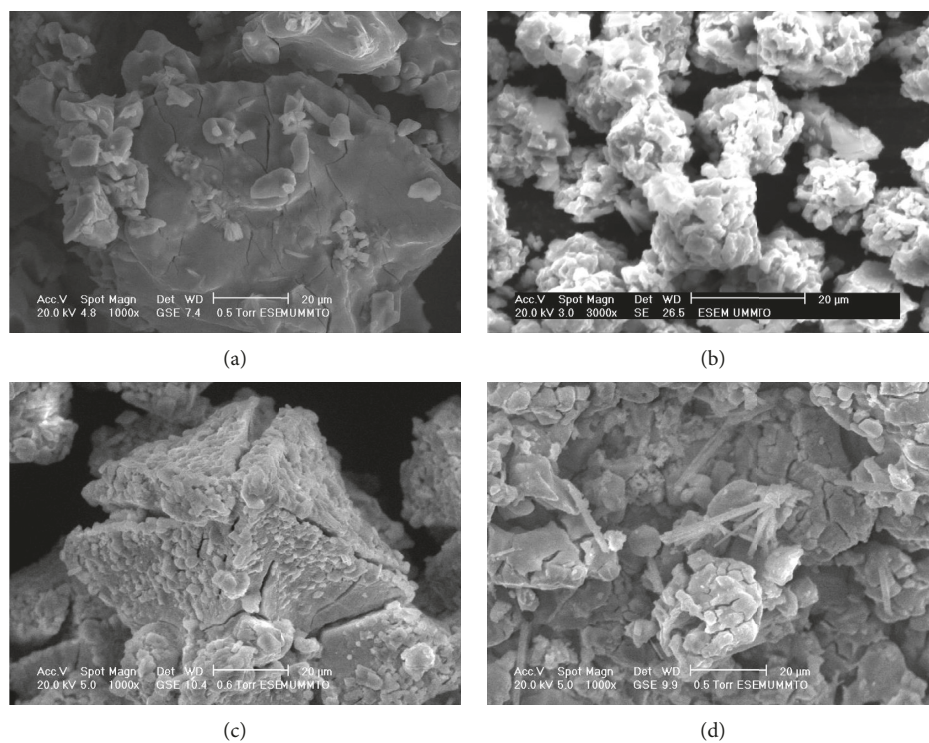


FIGURE 4: Scanning electron micrographs of (a) HPMo<sub>12</sub>; (b) FePMo<sub>12</sub>; (c) HPMo<sub>11</sub>V; (d) PMo<sub>11</sub>Fe.

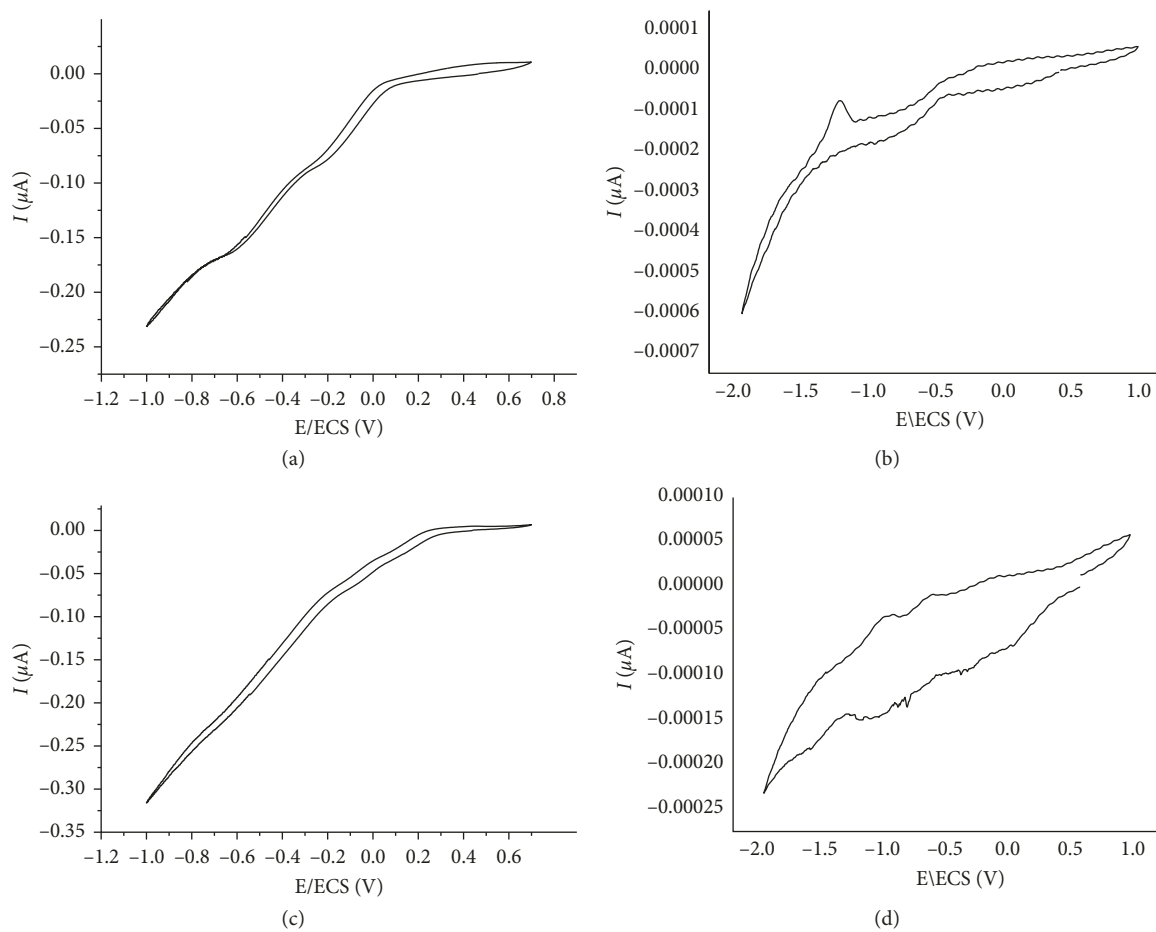


FIGURE 5: Voltamperograms of (a) HPMo<sub>12</sub>; (b) FePMo<sub>12</sub>; (c) HPMo<sub>11</sub>V; (d) PMo<sub>11</sub>Fe.

the vanadium (V/IV), iron (III/II), and molybdenum (VI/V, V/VI) couples, respectively, and followed by three reversible redox peaks at  $-0.90$ ,  $-1.61$ , and  $-1.8$  V for the  $\text{PMo}_{11}\text{V}$  and at  $-0.85$ ,  $-1.68$ , and  $-1.76$  for the  $\text{PMo}_{11}\text{Fe}$ . The redox properties of Keggin-type heteropolycompounds can be varied over a wide range by altering the chemical composition. In fact, the electron-accepting properties of Keggin anion are important for oxidative catalysis when electron transfer mechanisms are predominant. In other case, it is the ability of some oxygen atoms of the clusters or the possibility of being involved in complexation reactions that make them good catalysts for oxidation of hydrocarbons.

**3.1.6. Thermogravimetric Analysis.** The TGA profile for the thermal decomposition of the polyoxometalates is shown in Figure 6. The temperature at which their degradation starts depends on the protonation level and the composition of the polyoxometalates. It can be observed that the weight loss occurred in two steps in case of  $\text{HPMo}_{12}$ ,  $\text{HPMo}_{11}\text{V}$ , and  $\text{FePMo}_{12}$  samples and three steps in that of  $\text{PMo}_{11}\text{Fe}$  compounds. The first loss at low temperatures ( $<120^\circ\text{C}$ ) corresponds to the liberation of physisorbed water ( $12\text{--}13 \text{H}_2\text{O}$ ), and the second weight loss, between  $120^\circ\text{C}$  and  $380^\circ\text{C}$  results from the elimination of the three or four acid protons associated with 1.5 or 2 oxygen atoms of the POMs, leading to formation of an anhydride [38].

Their end product of thermal decomposition is the mixture of  $\text{MoO}_3$ ,  $\text{P}_2\text{O}_5$ , and  $\text{V}_2\text{O}_5$  (Scheme (1)), confirmed by X-ray diffraction and IR spectroscopy.

$\text{PMo}_{11}\text{Fe}$  exhibits high stability (Figure 6). It is known that the decomposition of  $(\text{NH}_4)_4\text{PMo}_{11}\text{FeO}_{39}$  begins even at  $175^\circ\text{C}$  and involves three stages in the process of transformation of  $(\text{NH}_4)_4\text{PMo}_{11}\text{FeO}_{39}$  into mixture oxides  $\text{P}_2\text{O}_5$ ,  $\text{MoO}_3$ , and  $\text{Fe}_2\text{O}_3$  (Scheme 2), located at approximately  $150^\circ\text{C}$ ,  $280^\circ\text{C}$ , and  $450^\circ\text{C}$ . The first peak is associated with removal of water from the polyoxometalate. The main decomposition peak at  $250^\circ\text{C}$  corresponds to the loss of constitution water. The third peak may be related to the decomposition of ammonium cations to ammonia and can be explained as shown.

**3.1.7. Acidic Properties of Polyoxometalates.** The gas-phase decomposition of isopropanol is an important probe reaction, as its product selectivity depends on the surface concentration of redox, basic, and acidic sites [39]. Redox sites or strong basic sites produce propanone by dehydrogenation reaction (a), whereas acidic sites give rise to propene and di-isopropylether, respectively [40], by dehydration reaction (b) (Figure 7).

The results obtained from the isopropanol decomposition using POMs as catalysts as a function of reaction temperature are presented in Table 1.

It is clear that  $\text{HPMo}_{11}\text{V}$  and  $\text{HPMo}_{12}$ , are the most active catalysts. The high activity can be correlated with increasing the surface acidity associated with the presence of protons in Keggin structure. Propene is the major reaction product. However, it is also observed that, when the protons in the parent acids ( $\text{H}_3\text{PMo}_{12}\text{O}_{40}$ ) are partially exchanged by iron

and ammonium cations,  $[(\text{NH}_4)_{2.5}\text{Fe}_{0.1}\text{H}_{0.2}\text{PMo}_{12}\text{O}_{40}]$  improves the catalytic activity (Table 1). This can be attributed to the partial hydrolysis of the polyanion during preparation, which formed weakly acidic  $\text{H}^+$ . On the contrary, when the iron is in anionic position ( $\text{PMo}_{11}\text{Fe}$ ), the initial activity decreased, resulting in conversion relatively lower than the iron in cationic position ( $\text{FePMo}_{12}$ ). This decrease attributed to the decrease in the number and the strength of the acid sites of the catalyst. The presence of redox species  $\text{Mo}^{\text{VI}}/\text{Mo}^{\text{IV}}$ ,  $\text{V}^{\text{V}}/\text{V}^{\text{IV}}$ , and  $\text{Fe}^{\text{III}}/\text{Fe}^{\text{II}}$  in the catalysts can contribute to dehydration and dehydrogenation in the decomposition of isopropanol.

### 3.2. Catalytic Test

**3.2.1. Catalytic Activity.** The effect of reaction temperature for the partial oxidation of toluene over polyoxometalates was estimated at  $250^\circ\text{C}$ ,  $300^\circ\text{C}$ , and  $350^\circ\text{C}$ . The toluene conversion and the product selectivity in a  $\text{CO}_2$  atmosphere at time on stream of 8 h are shown in Table 2. The toluene conversion increased with increasing temperature for all catalysts. However, high temperatures also enhance an undesired parallel process, dealkylation reaction (benzene and methane) that reduces the selectivity to the desired product (benzyl alcohol or benzaldehyde).

In the reaction with the  $\text{H}_3\text{PMo}_{12}\text{O}_{40}$  catalyst, the toluene conversion increased from 7 to 52.3% with an increase in the reaction temperature from  $250^\circ\text{C}$  to  $350^\circ\text{C}$ . The benzaldehyde selectivity decreased from 63% at  $250^\circ\text{C}$  to 36.0% at  $350^\circ\text{C}$ , that of benzene (dealkylation product) increased from 37% to 64%. Hence, higher temperatures cause higher dealkylation of toluene and formation of lower amounts of benzaldehyde. At all temperatures,  $\text{HPMo}_{11}\text{V}$  displayed very similar conversion than  $\text{HPMo}_{12}$  but is more selective towards benzaldehyde (80–67% selectivity) benzyl alcohol was also observed as a minor product. These results are in accord with those obtained by other authors which have demonstrated that the use of vanadium-containing polyoxometalates improved catalytic performances (conversion and selectivity) as in the case of isobutane oxidation [29, 41]. On the other hand, it was reported that both  $\text{V}^{5+}$  and  $\text{V}^{4+}$  species were likely the active sites in the selective oxidation of toluene to benzaldehyde [42]. In the case of  $\text{H}_4\text{PMo}_{11}\text{VO}_{40}$ , the reduction of  $\text{V}^{5+}$  to  $\text{V}^{4+}$  is very quick leading to stability of benzaldehyde selectivity from the beginning of the reaction. This agrees with the obtained results by Cavani et al., in oxidative isobutane [43]; the presence of vanadium will accelerate the reduction of compound suggesting that  $\text{V}^{4+}$  species act as reducing species towards  $\text{Mo}^{6+}$  leading to  $\text{Mo}^{5+}$  and  $\text{V}^{5+}$  species. In the reaction with the  $\text{FePMo}_{12}$  catalyst (Table 2), toluene conversion is similar to that of the  $\text{HPMo}_{12}$  catalyst observed. The benzaldehyde selectivity at the reaction temperature of  $250^\circ\text{C}$  is below 40%, which has been decreased to approximately 30% and 21% with an increase in the reaction temperature from  $250^\circ\text{C}$  to  $300^\circ\text{C}$  and  $350^\circ\text{C}$ , respectively. However, the benzyl alcohol selectivity remained constant in the range between  $250^\circ\text{C}$  and  $350^\circ\text{C}$ . Higher benzene selectivity is observed at all

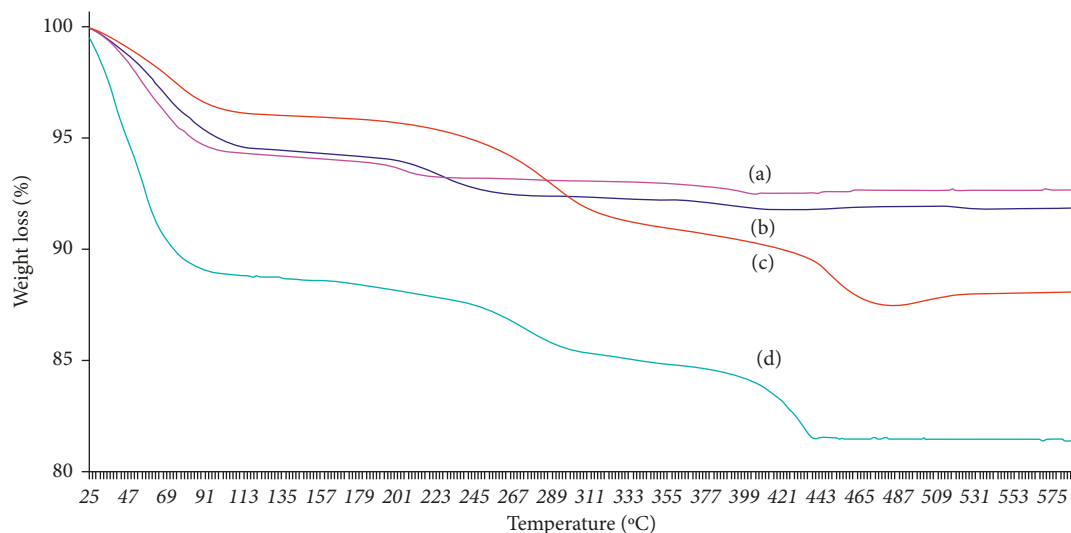
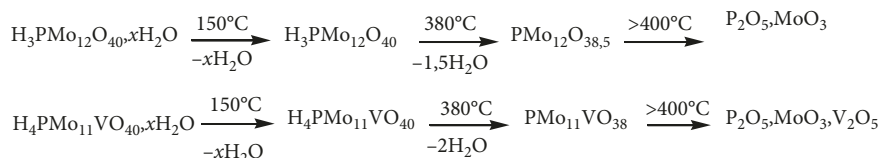
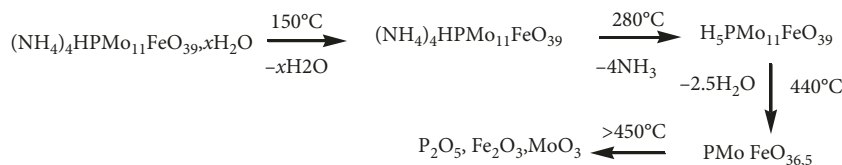


FIGURE 6: The TGA profiles of (a)  $\text{HPMo}_{12}$ ; (b)  $\text{HPMo}_{11}\text{V}$ ; (c)  $\text{FePMo}_{11}$ ; (d)  $\text{PMo}_{11}\text{Fe}$ .



SCHEME 1: Thermal decomposition process of  $\text{HPMo}_{12}$  and  $\text{HPMo}_{11}\text{V}$ .



SCHEME 2: Thermal decomposition process of  $\text{PMo}_{11}\text{Fe}$ .

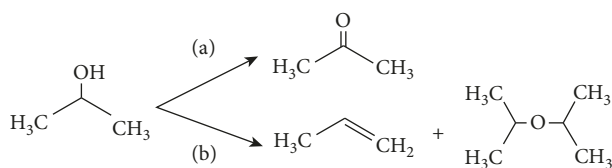


FIGURE 7: Isopropanol decomposition on acid and redox sites.

reaction temperatures. The obtained results indicated that the selectivity of benzene increases with increasing temperature; thus,  $\text{FePMo}_{12}$  surface has strong acidic sites, which is evident from the higher dealkylation process than dehydrogenation; these results agree with those observed in dehydrogenation of isopropanol to propene. The same products (benzyl alcohol, benzaldehyde, and benzene) are obtained with  $\text{PMo}_{11}\text{Fe}$ , and the results are listed in Table 2. Generally, the conversion of toluene into oxidized products was much more efficient than for the catalysts listed in Table 2. With  $\text{PMo}_{11}\text{Fe}$ , conversion of toluene is more important and becomes highly selective to the formation of benzyl alcohol at low temperatures. The catalyst

also gave benzene but only as a minor product, benzaldehyde being the major one. This is suggested that iron in anionic position decreases the acidity and accelerates more the redox process. The results for  $\text{PMo}_{11}\text{Fe}$  show that the conversion of toluene to oxygenate products (benzyl alcohol + benzaldehyde) is higher than the dealkylation process (benzene) indicating the redox of  $\text{PMo}_{11}\text{Fe}$  surface. The easy redox cycle between oxidized and reduced iron species ( $\text{Fe}^{3+}/\text{Fe}^{2+}$ ) generates a highly active catalyst.

**3.2.2. Reaction Kinetics.** A kinetic study of toluene partial oxidation was performed at  $200^\circ\text{C}$  over  $\text{PMo}_{11}\text{Fe}$ , with a total flow rate of 50 ml/min and catalyst weight of 200 mg. The reaction rate of toluene oxidation by carbon dioxide was given by

$$r = kP^{\alpha}\text{toluene} P^{\beta}\text{CO}_2, \quad (1)$$

where  $\alpha$  and  $\beta$  are the partial order of toluene and carbon dioxide.

TABLE 1: Catalytic activity of catalysts at different temperatures in isopropanol decomposition.

Catalysts	T (°C)	Conversion (%)	Products selectivities (%)		
			Propylene	Di-isopropylether	Acetone
H <sub>3</sub> PMo <sub>12</sub> O <sub>40</sub>	100	17	60	30	10
	150	60	80	13	7
	200	90	92	4	4
H <sub>4</sub> PMo <sub>11</sub> VO <sub>40</sub>	100	19	56	16	28
	150	65	84	6	10
	200	97	90	2	8
FePMo <sub>12</sub> O <sub>40</sub>	100	10	72	20	8
	150	80	90	9	1
	200	95	98	1	1
PMo <sub>11</sub> FeO <sub>39</sub>	100	5	15	5	80
	150	32	35	3	62
	200	45	69	1	30

TABLE 2: Effect of reaction temperature on the partial oxidation of toluene with CO<sub>2</sub> over polyoxometalates.

Catalysts	T (°C)	Conversion (%)	Products' selectivity (%)		
			C <sub>6</sub> H <sub>6</sub>	C <sub>6</sub> H <sub>5</sub> -CH <sub>2</sub> OH	C <sub>6</sub> H <sub>5</sub> -CHO
H <sub>3</sub> PMo <sub>12</sub> O <sub>40</sub>	250	7	37	—	63
	300	14.5	51	—	49
	350	52.3	64	—	36
H <sub>4</sub> PMo <sub>11</sub> VO <sub>40</sub>	250	6.1	12	8	80
	300	16.4	18	10	72
	350	54.7	31	2	67
PMo <sub>11</sub> Fe	200	5	30	65	5
	250	26	25	50	25
	300	44.4	20	32	48
	350	75.4	19	15	66
FePMo <sub>12</sub>	250	14	39	21	40
	300	31.0	51	19	30
	350	55.1	61	18	21

The value of these orders can then be obtained by linearizing this equation and by plotting the corresponding logarithmic curves:

$$\ln r = \ln k + \alpha \ln(P_{\text{toluene}}) + \beta \ln(P_{\text{CO}_2}). \quad (2)$$

In most cases, a constant carbon dioxide pressure of 50 Torr was used in the first set of experiments as the pressure of the toluene was varied from 2.5 to 25 Torr (Figure 8(a)), and the Ph-CH<sub>3</sub> pressure was fixed at 5 Torr while the CO<sub>2</sub> pressure was changed from 50 to 100 Torr in the second (Figure 8(b)).

The results indicated a reaction of zero order with respect to carbon dioxide and first order with respect to toluene.

These orders suggested the reaction was of the Mars and van Krevelen type, with the rate-determining step being the reduction of the catalyst surface by the hydrocarbon [44].

According to the Mars and van Krevelen model, the reaction of toluene partial oxidation occurs in two steps: the oxidation of toluene by the oxidized catalyst (3) and the reoxidation of reduced catalyst (4).



In these equations SO, S,  $k_{(\text{red})}$ , and  $k_{(\text{ox})}$ , respectively, represent the oxidized and reduced sites of the catalysts, the rate constants of the reduction, and oxidation stages of the catalyst. The rate of steps (3) and (4) would then be

$$\begin{aligned} r(\text{red}) &= k_{(\text{red})} P_{\text{toluene}} [\text{SO}] \\ r(\text{ox}) &= k_{(\text{ox})} P_{\text{CO}_2} [\text{S}] \end{aligned} \quad (5)$$

In steady state, these rates are equal:  $r = r(\text{red}) = r(\text{ox})$ .

Moreover, the material balance corresponding to the reaction sites is  $[\text{SO}] + [\text{S}] = [\text{S}]_0$ ;  $[\text{SO}]$ ,  $[\text{S}]$ , and  $[\text{S}]_0$  are, respectively, the concentrations of the oxidized, reduced, and total sites. The resolution of the system of equations above makes it possible to obtain the expression of the rate of reaction in steady state:

$$r = \frac{k_{(\text{red})} P_{\text{toluene}} \times k_{(\text{ox})} P_{\text{CO}_2}^n}{k_{(\text{red})} P_{\text{toluene}} + k_{(\text{ox})} P_{\text{CO}_2}^n} \times [\text{S}]_0. \quad (6)$$

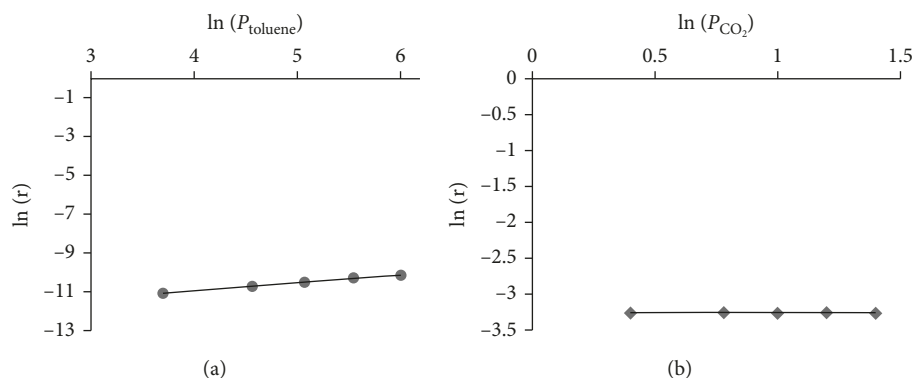


FIGURE 8: Reaction order of partial oxidation of toluene by carbon dioxide.

If  $[S]_0 = 1$ :

$$r = \frac{k_{(\text{red})}P_{\text{toluene}} \times k_{(\text{ox})}P_{\text{CO}_2}^n}{k_{(\text{red})}P_{\text{toluene}} + k_{(\text{ox})}P_{\text{CO}_2}^n} \quad (7)$$

If the reduction step is limiting, it is possible to write  $k_{(\text{ox})} \gg k_{(\text{red})} P_{\text{CO}_2}$ .

Hence,  $r \cong k_{(\text{red})} P_{\text{toluene}} = k P_{\text{toluene}}$ , where  $k$  is the rate constant of the global process. The kinetics is indeed of the first order with respect to the toluene.

Moreover, the values of the rate constants of the reduction and reoxidation steps were determined graphically by linearizing the equation of the overall rate:

$$\frac{1}{r} = \frac{1}{k} (\text{red})P_{\text{toluene}} + \frac{1}{k} (\text{ox})P_{\text{CO}_2} \quad (8)$$

The plotting of the corresponding curves at constant pressure of toluene or carbon dioxide leads to the following values:  $k_{(\text{red})} = 4,1 \cdot 10^{-4} \text{ mol} \cdot \text{min}^{-1} \cdot \text{g}^{-1} \cdot \text{Torr}^{-1}$  and  $k_{(\text{ox})} = 0,50 \text{ mol} \cdot \text{min}^{-1} \cdot \text{g}^{-1} \cdot \text{Torr}^{-1}$ . This conclusion was in good agreement with the decomposition of isopropanol (Table 2) and cyclic voltammetry studies showing the redox properties of the  $\text{PMo}_{11}\text{Fe}$  catalyst. Since  $k_{(\text{red})} \ll k_{(\text{ox})}$ , the limiting step of the reaction is the reoxidation of the catalyst as found by Van Der Wiele et al. [21]. In initial kinetic conditions, only benzyl alcohol and benzaldehyde as oxygenate products were detected. Besides, when the contact time tended to zero, the  $\text{C}_6\text{H}_5\text{-CH}_3\text{OH}/\text{C}_6\text{H}_5\text{-CHO}$  ( $\gamma$ ) or  $\text{C}_6\text{H}_5\text{-CHO}/\text{C}_6\text{H}_5\text{-CH}_3\text{OH}$  ( $1/\gamma$ ) ratios tended towards zero or an infinite value, respectively (Figure 9). These trends suggested that benzyl alcohol was an intermediate in benzaldehyde formation, as shown by the following reaction pathway:



The same trend was observed during the study of the effect of the reaction temperature on the product selectivities.

Figure 10 shows that selectivity of benzyl alcohol decreases as the temperature increases, while benzaldehyde selectivity increases with reaction temperature. This result confirmed that benzyl alcohol was a precursor in benzaldehyde formation.

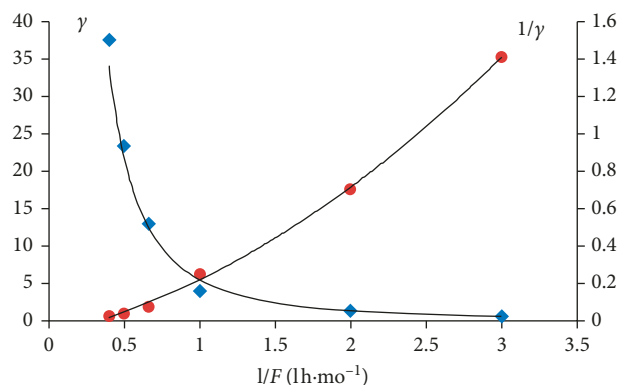


FIGURE 9: Effect of the contact time on the relative selectivities in the partial oxidation of toluene at 200°C over  $\text{PMo}_{11}\text{Fe}$ .

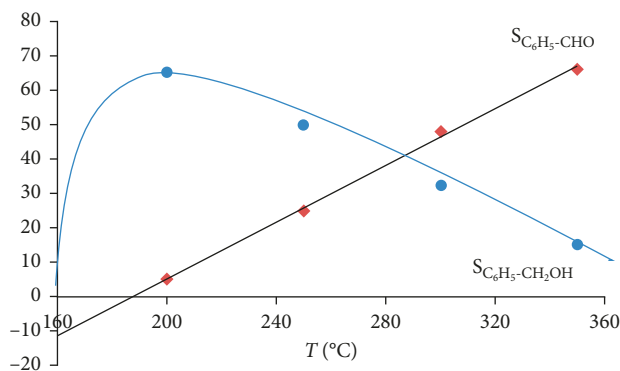


FIGURE 10: Effect of the reaction temperature on the selectivities in the partial oxidation of toluene over  $\text{PMo}_{11}\text{Fe}$ .

Activation energy of the catalytic oxidation of toluene to benzaldehyde, using  $\text{CO}_2$  as oxidant, was determined from the plot of  $\ln k$  against  $1/T$  (Figure 11). The activation energy was calculated using the following equation: slope =  $-E_a/R$ , where  $E_a$  is activation energy,  $R$  is the gas constant. The value of activation energy was found to be 62.639 KJ/mol.

3.2.3. Mechanism and Pathway of Toluene Partial Oxidation by  $\text{CO}_2$ . It has been well recognized that the selective

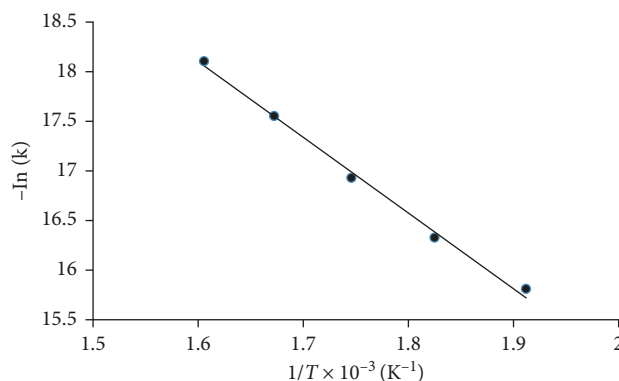


FIGURE 11: Arrhenius plot for determination of activation energy.

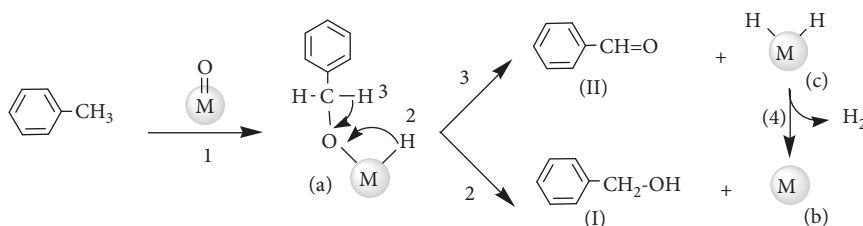


FIGURE 12: Proposed mechanism for the partial oxidation of toluene on M=O centers.

oxidation of toluene proceeded via a van Krevelen redox mechanism [44], but the pathways and product distribution depended on the nature of catalysts and the reaction conditions. For toluene partial oxidation to benzyl alcohol and benzaldehyde using carbon dioxide as oxidant, the most strongly supported mechanism consists of a consecutive conversion scheme  $C_6H_5-CH_3 \rightarrow C_6H_5-CH_2OH \rightarrow C_6H_5-CHO$ . This indicates that benzyl alcohol can be formed as a precursor of benzaldehyde in the catalytic oxidation of toluene over a transition metallic oxide catalyst. According to the widely accepted mechanism of partial oxidation of toluene by  $CO_2$ , the breaking of the C–H bond in the toluene is the rate-determining step [45]. In the case of the catalytic partial oxidation of toluene by  $CO_2$  over polyoxometalate catalysts, the formation of benzaldehyde and benzyl alcohol during the toluene adsorption suggests that toluene is activated by abstracting a hydrogen atom from the methyl group. This is followed by the bonding of the lattice oxygen nearby over the M=O centers with the primary carbon of benzyl species leading to the formation of benzyloxy species (a). This is in agreement with the work of Busca et al. [46]. They studied by IR spectroscopy the interaction of light hydrocarbons over the  $MgCr_2O_4$ . It has been concluded that every hydrocarbon reacts at its weakest C–H bond giving rise to the corresponding alkoxide species. In the first step of the mechanism,  $C_6H_5-CH_3$  adsorbed on the M=O centers to form an benzyloxy species ( $C_6H_5-CH_2-O-M-H$ ) (a) (Step 1). Benzyl alcohol (I) is then formed via the transfer of a hydrogen atom from the hybrid group to the benzyloxy (Step 2). Surface benzyloxy groups decompose to the adsorbed  $C_6H_5-CHO$ ; desorption of benzaldehyde (II) and dihydrogen lead to the final products and a reduced catalyst surface (Step 3). The pathway for the oxidation of toluene over polyoxometalates is shown in the reaction scheme Figure 12.

Reoxidation of the catalyst by  $CO_2$  restores the lattice oxygen atom of the M metal, then the M=O centers are reestablished for the next turnover cycle. This sequence is represented by (Figure 13)

Toluene, when passed over different heteropolycompound catalysts at  $250^\circ C-400^\circ C$ , has been found to yield benzyl alcohol and benzaldehyde in addition to the hydrodealkylation [47] products benzene (III) and methane (IV). Here, the toluene reacts with the adsorbed hydrogen to produce benzene and methane as shown in Figure 14.

#### 4. Conclusion

Both IR spectroscopy and X-ray diffraction indicate for  $FePMo_{12}$  and  $PMo_{11}Fe$  salts, the presence of a single crystalline phase, and IR spectra typical of the Keggin anion; TGA shows that the salts containing iron are more stable than the pure acidic  $H_3PMo_{12}O_{40}$  and  $H_4PMo_{11}VO_{40}$ . These results show also that the vanadium and iron play a very important role in benzaldehyde selectivity and indicate clearly that the substitution of protons by  $NH_4^+$  and  $Fe^{3+}$  cations or  $Mo^{6+}$  by  $V^{5+}$  and  $Fe^{3+}$  induced important changes in the acid-base and oxidoreduction properties of phosphomolybdate heteropolyanions of Keggin structure. In this study,  $PMo_{11}V$  and  $PMo_{11}Fe$  catalyzed the toluene partial oxidation with carbon dioxide as an oxidant to the corresponding oxygenate compounds efficiently and selectively.

The partial oxidation of toluene selectively produced oxygenated compounds besides benzene. The reaction orders were 1 and 0 in toluene and carbon dioxide, respectively. The overall process seemed to obey a redox mechanism of Mars and van Krevelen type, in which the reduction step would be rate determining. Benzyl alcohol

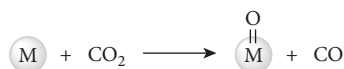


FIGURE 13



FIGURE 14: Toluene hydrodealkylation.

appeared as the reaction intermediate in benzaldehyde formation.

## Data Availability

The data used to support the findings of this study are included within the article.

## Conflicts of Interest

The authors declare that they have no conflicts of interest.

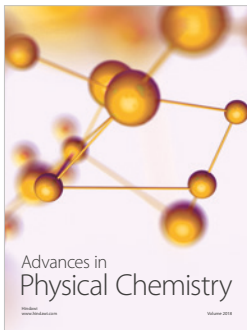
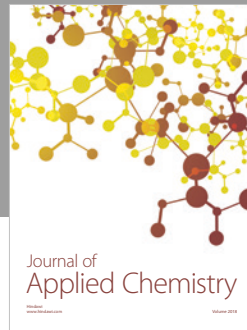
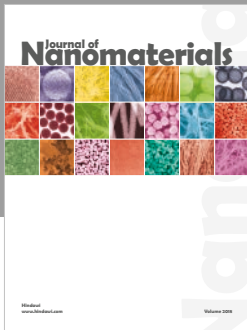
## Supplementary Materials

The supplementary materials for this work contain the detailed method of preparation of pure acids  $\text{H}_3\text{PMo}_{12}\text{O}_{40}$  and  $\text{H}_4\text{PMo}_{11}\text{VO}_{40}$  and heteropolysalts  $(\text{NH}_4)_{2.5}\text{Fe}_{0.08}\text{H}_{0.26}\text{PMo}_{12}\text{O}_{40}$  and  $(\text{NH}_4)_4\text{PMo}_{11}(\text{H}_2\text{O})\text{FeO}_{39}$  with iron outside and inside Keggin structure, respectively. The supplementary materials include the expressions of toluene conversion and products' selectivities. (*Supplementary Materials*)

## References

- [1] A. I. Appelbaum, "Process of manufacturing benzaldehyde," US Patent 1302273A, 1918.
- [2] M. L. Kantem, B. M. Choudary, P. Sreekanth, and K. K. Rao, "Process for the production of benzaldehyde by the catalytic liquid phase air oxidation of toluene," US Patent 6495726, 2002.
- [3] D. Haen, 1901 German Patent 128616 (1900), US Patent 687834.
- [4] P. Ciambelli, L. Lisi, G. Ruoppolo, G. Russo, and J. C. Volta, "Oxidative dehydrogenation of ethane over vanadium and niobium oxides supported catalysts," *Studies in Surface Science and Catalysis*, vol. 110, pp. 285–294, 1997.
- [5] X. Gao, M. A. Banares, and I. E. Wachs, "Ethane and n-butane oxidation over supported vanadium oxide catalysts: an in situ UV-visible diffuse reflectance spectroscopic investigation," *Journal of Catalysis*, vol. 188, no. 2, pp. 325–331, 1999.
- [6] M. Chaar, D. Patel, and H. H. Kung, "Selective oxidative dehydrogenation of propane over  $\text{V}_2\text{O}_5\text{-MoO}_3/\gamma\text{-Al}_2\text{O}_3$  catalysts," *Journal of Catalysis*, vol. 109, no. 2, pp. 463–467, 1988.
- [7] T. Blasco and J. M. L. Nieto, "Oxidative dehydrogenation of short chain alkanes on supported vanadium oxide catalysts," *Applied Catalysis A: General*, vol. 157, no. 1–2, pp. 117–142, 1997.
- [8] G. Deo and I. E. Wachs, "Reactivity of supported vanadium oxide catalysts: the partial oxidation of methanol," *Journal of Catalysis*, vol. 146, no. 2, pp. 323–334, 1994.
- [9] N. E. Quaranta, J. Soria, V. C. Corberán, and J. L. G. Fierro, "Selective oxidation of ethanol to acetaldehyde on  $\text{V}_2\text{O}_5/\text{TiO}_2/\text{SiO}_2$  catalysts," *Journal of Catalysis*, vol. 171, no. 1, pp. 1–13, 1997.
- [10] S. Velusamy and T. Punniyamurthy, "Novel vanadium-catalyzed oxidation of alcohols to aldehydes and ketones under atmospheric oxygen," *Organic Letters*, vol. 6, no. 2, pp. 217–219, 2004.
- [11] Q. Sun, J.-M. Jehng, H. Hu, R. G. Herman, and K. Klier, "SituRaman spectroscopy during the partial oxidation of methane to formaldehyde over supported vanadium oxide catalysts," *Journal of Catalysis*, vol. 165, pp. 91–101, 1997.
- [12] K. G. Fang, B. Wang, and Y. H. Sun, "Partial oxidation of toluene on  $\text{VO}_x\text{-TiO}_x/\text{SBA-15}$ ," *Chemical Research in Chinese Universities*, vol. 25, no. 6, pp. 924–928, 2009.
- [13] H. Ge, G. Chen, Q. Yuan, and H. Li, "Gas phase catalytic partial oxidation of toluene in a microchannel reactor," *Catalysis Today*, vol. 110, pp. 171–178, 2005.
- [14] J. W. Yoon, S. H. Jhung, and J. S. Chang, "Vapor-phase oxidation of alkylaromatics over  $\text{V}/\text{TiO}_2$  and  $\text{VSb}/\text{Al}_2\text{O}_3$  catalysts: effect of alkali metals," *Bull Korean Chemical Society*, vol. 28, no. 12, pp. 2405–2408, 2007.
- [15] N. Nag, T. Fransen, and P. Mars, "The oxidation of toluene on various molybdenum-containing catalysts," *Journal of Catalysis*, vol. 68, pp. 77–85, 1981.
- [16] I. S. Tomskii, M. V. Vishnetskaya, and A. I. Kokorin, "The partial catalytic oxidation of toluene on vanadium and molybdenum oxides," *Russian Journal Physics Chemical B*, vol. 2, no. 4, pp. 562–567, 2008.
- [17] P. C. Van Geem and A. J. J. M. Teunissen, "Catalytic gas phase oxidation of toluene to benzaldehyde and/or benzoic acid," 1979, US Patent 4,137,259.
- [18] S. Larrondo, A. Barbaro, B. Irigoyen, and N. Amadeo, "Oxidation of toluene to benzaldehyde over  $\text{VSb}_{0.8}\text{Ti}_{0.2}\text{O}_4$ : effect of the operating conditions," *Catalysis Today*, vol. 64, pp. 179–187, 2001.
- [19] C. Subrahmanyama, B. Louis, F. Rainone, B. Viswanathan, A. Renken, and T. K. Varadarajan, "Catalytic oxidation of toluene with molecular oxygen over Cr-substituted mesoporous materials," *Applied Catalysis A General*, vol. 241, pp. 205–215, 2003.
- [20] K. Papadatos, "Catalyst screening using a stone DTA apparatus: oxidation of toluene over cobalt-metal oxide catalysts," *Journal of Catalysis*, vol. 123, pp. 116–123, 1973.
- [21] K. Van Der Wiele and P. J. Van Den Berg, "Oxidation of toluene over bismuth molybdate catalysts," *Journal of Catalysis*, vol. 39, pp. 437–448, 1975.
- [22] M. Xue, X. Gu, J. Chen, H. Zhang, and J. Shen, "Characterization of acidic and redox properties of Ce-Mo-O catalysts for the selective oxidation of toluene," *Thermochimica Acta*, vol. 434, pp. 50–54, 2005.
- [23] C. Perdomo, A. Pérez, R. Molina, and S. Moreno, "Storage capacity and oxygen mobility in mixed oxides from transition metals promoted by cerium," *Applied Surface Science*, vol. 383, pp. 42–48, 2016.
- [24] N. Mizuno, M. Tateishi, and M. Iwamoto, "Oxidation of isobutane catalyzed by  $\text{Cs}_x\text{H}_{3-x}\text{PMo}_{12}\text{O}_{40}$ -based heteropoly compounds," *Journal of Catalysis*, vol. 163, no. 1, pp. 87–94, 1996.
- [25] S. Hocine, C. Rabia, M. M. Bettahar, and M. Fournier, "Oxidative dehydrogenation of cyclohexane over heteropolymolybdates,"

- Studies in Surface Sciences and Catalysis*, vol. 130, pp. 1895–1900, 2000.
- [26] F. Cavani, M. Koutyrev, and F. Trifirò, “Oxidative dehydrogenation of ethane to ethylene over antimony-containing Keggin-type heteropolyoxomolybdates,” *Catalysis Today*, vol. 24, no. 3, pp. 365–368, 1995.
- [27] N. Dimitratos and J. C. Vadrine, “Role of acid and redox properties on propane oxidative dehydrogenation over polyoxometallates,” *Catalysis Today*, vol. 81, no. 4, pp. 561–571, 2003.
- [28] S. Mansouri, O. Benlounes, C. Rabia, R. Thouvenot, M. M. Bettahar, and S. Hocine, “Partial oxidation of methane over modified Keggin-type polyoxotungstates,” *Journal of Molecular Catalysis A Chemical*, vol. 379, pp. 255–262, 2013.
- [29] G. Busca, F. Cavani, E. Etienne et al., “Reactivity of Keggin-type heteropolycompounds in the oxidation of isobutane to methacrolein and methacrylic acid: reaction mechanism,” *Journal of Molecular Catalysis A*, vol. 114, no. 1-3, pp. 343–359, 1996.
- [30] H. S. Jiang, X. Mao, S. J. Xie, and B. K. Zhong, “Partially reduced heteropoly compound catalysts for the selective oxidation of propane,” *Journal of Molecular Catalysis A*, vol. 185, no. 1-2, pp. 143–149, 2002.
- [31] Z. Zhang, Z. Zhao, and C. Xu, “Research advances in the catalysts for the selective oxidation of ethane to aldehydes,” *Chinese Science Bulletin*, vol. 50, no. 9, pp. 833–840, 2005.
- [32] R. Bulánek and K. Novoveská, “Oxidative dehydrogenation of propane by nitrous oxide and/or oxygen over Co beta zeolite,” *Reaction Kinetic and Catalysis Letters*, vol. 80, no. 2, pp. 337–343, 2003.
- [33] K. Nakagawa, K. Okumura, T. Shimamura et al., “Novel selective oxidation of light alkanes using carbon dioxide. Oxidized diamond as a novel catalytic medium,” *Chemical Letters*, vol. 32, no. 9, pp. 866–867, 2003.
- [34] J. S. Yoo, “Selective gas-phase oxidation at oxide nanoparticles on microporous materials,” *Catalysis Today*, vol. 41, no. 4, pp. 409–432, 1998.
- [35] G. A. Tsigdinos, “Preparation and characterization of 12-molybdophosphoric and 12-molybdosilicic acids and their metal salt,” *Industrial & Engineering Chemistry Product Research and Development journal*, vol. 13, no. 4, pp. 267–274, 1974.
- [36] N. Mizuno, J.-S. Min, and A. Taguchi, “Preparation and characterization of  $\text{Cs}_{2.5}\text{H}_{1.2}\text{PMo}_{11}\text{Fe}(\text{H}_2\text{O})\text{O}_{39}\cdot 6\text{H}_2\text{O}$  and investigation of effects of iron-substitution on heterogeneous oxidative dehydrogenation of 2-propanol,” *Chemical Materials journal*, vol. 16, no. 14, pp. 2819–2825, 2004.
- [37] C. Rocchiccioli-Deltcheff, R. Thouvenot, R. Franck et al., “Spectres i.r. Raman d’hétéropolyanions  $\alpha\text{-XM}_{12}\text{O}_{40}^{n-}$  de structure de type Keggin (X = B<sup>III</sup>, Si<sup>IV</sup>, Ge<sup>IV</sup>, P<sup>V</sup>, As<sup>V</sup> et M = W<sup>VI</sup> et Mo<sup>VI</sup>),” *Spectrochimica Acta*, vol. 32, no. 3, pp. 587–597, 1976.
- [38] C. Marchal-Roch, R. Bayer, J. F. Moisan, A. Tézé, and G. Hervé, “Oxidative dehydrogenation of isobutyric acid: characterization and modeling of vanadium containing polyoxometalate catalysts,” *Topics in Catalysis*, vol. 3, no. 3-4, pp. 407–419, 1996.
- [39] A. Gervasin, J. Fenyvesi, and A. Auroux, “Study of the acidic character of modified metal oxide surfaces using the test of isopropanol decomposition,” *Catalysis Letters*, vol. 43, no. 3-4, pp. 219–228, 1997.
- [40] M. Ai and S. Suzuki, “The acid-base properties of  $\text{MoO}_3\text{-Bi}_2\text{O}_3\text{-P}_2\text{O}_5$  catalysts and their correlation with catalytic activity and selectivity,” *Journal of Catalysis*, vol. 40, no. 2, pp. 203–211, 1975.
- [41] N. Mizuno, M. Tateishi, and M. Iwamoto, “Enhancement of catalytic activity of  $\text{Cs}_{2.5}\text{Ni}_{0.08}\text{H}_{0.34}\text{PMo}_{12}\text{O}_{40}$  by V<sup>5+</sup>-substitution for oxidation of isobutane into methacrylic acid,” *Applied Catalysis A*, vol. 118, no. 1, pp. L1–L4, 1994.
- [42] T. Zhang, L. Mao, and W. Liu, “Gas phase selective catalytic oxidation of toluene to benzaldehyde on  $\text{V}_2\text{O}_5\text{-Ag}_2\text{O}/\eta\text{-Al}_2\text{O}_3$  catalyst,” *Journal of Natural Gas Chemistry*, vol. 13, pp. 238–243, 2004.
- [43] F. Cavani, R. Mezzogori, A. Pigamo, F. Trifiro, and E. Etienne, “Main aspects of the selective oxidation of isobutane to methacrylic acid catalyzed by Keggin-type polyoxometalates,” *Catalysis Today*, vol. 71, no. 1-2, pp. 97–110, 2001.
- [44] P. Mars and D. W. Van Krevelen, “Oxidations carried out by means of vanadium oxide catalysts,” *Chemical Engineering Science*, vol. 3, pp. 41–49, 1954.
- [45] K. Chen, A. Khodakov, J. Young, A. T. Yang, and E. Iglesia, “Isotopic tracer and kinetic studies of oxidative dehydrogenation pathways on vanadium oxide catalysts,” *Journal of Catalysis*, vol. 186, no. 2, pp. 325–333, 1999.
- [46] G. Busca, E. Finocchio, V. Lorenzelli, G. Ramis, and M. Baldi, “IR studies on the activation of C-H hydrocarbon bonds on oxidation catalysts,” *Catalysis Today*, vol. 49, no. 4, pp. 453–465, 1999.
- [47] P. A. Simell, J. O. Hepola, and A. O. I. Krause, “Effects of gasification gas components on tar and ammonia decomposition over hot gas cleanup catalysts,” *Fuel*, vol. 76, no. 12, pp. 1117–1127, 1997.



Hindawi

Submit your manuscripts at  
[www.hindawi.com](http://www.hindawi.com)

